PERGAMON

Vision Research 41 (2001) 3353–3369

Vision Research

www.elsevier.com/locate/visres

Plasticity of convergence-dependent variations of cyclovergence with vertical gaze

C.M. Schor *, J.S. Maxwell, E.W. Graf

School of Optometry, University of California, Berkeley CA 94720-2020, USA

Received 20 September 2000; received in revised form 16 March 2001

Abstract

Binocular alignment of foveal images is facilitated by cross-couplings of vergence eye movements with distance and direction of gaze. These couplings reduce horizontal, vertical and cyclodisparities at the fovea without using feedback from retinal image disparity. Horizontal vergence is coupled with accommodation. Vertical vergence that aligns tertiary targets in asymmetric convergence is thought to be coupled with convergence and horizontal gaze. Cyclovergence aligns the horizontal retinal meridians during gaze elevation in symmetrical convergence and is coupled with convergence and vertical gaze. The latter vergence-dependent changes of cyclovergence have been described in terms of the orientation of Listing's plane and have been referred to as the binocular extension of Listing's law. Can these couplings be modified? Plasticity has been demonstrated previously for two of the three dimensions of vergence (horizontal and vertical). The current study demonstrates that convergence-dependent changes of the orientation of Listing's plane can be adapted to either exaggerate or to reduce the cyclovergence that normally facilitates alignment of the horizontal meridians of the retinas with one another during gaze elevation in symmetrical convergence. The adaptability of cyclovergence demonstrates a neural mechanism that, in conjunction with the passive forces determined by biomechanical properties of the orbit, could play an active role in implementing Listing's extended law and provide a means for calibrating binocular eye alignment in three dimensions.

Keywords: Plasticity; Cyclovergence; Convergence; Vertical gaze; Listing's law

1. Introduction

The oculomotor system can align the two eyes without utilizing visual feedback from retinal image disparity by cross-coupling vergence in three dimensions with distance and direction of gaze. Horizontal disparity at the fovea is reduced by convergence that is scaled inversely with viewing distance and by a coupling with accommodation (Alpern & Ellen, 1956). Vertical disparity subtended by elevated targets viewed in asymmetric convergence is reduced by vertical vergence that is scaled with convergence and horizontal gaze eccentricity (assuming a non-Helmholtz coordinate system: see Collewijn, 1994; Schor, Maxwell, & Stevenson, 1994; Ygge & Zee, 1995). Cyclodisparity of elevated targets viewed in symmetrical convergence is reduced by torsional alignment of the horizontal meridians of the retinas with the visual plane (Allen & Carter, 1967; Mok, Cadera, Ro, Crawford, & Vilis, 1992; Van Rijn, Van der Steen, & Collewijn, 1994; Tweed, 1997; Somani, Desouza, Tweed, & Vilis, 1998). This cyclovergence (Cv) is scaled (K) with combinations of convergence (C) and vertical eye position (V) where

$$K = Cv/(C*V/2) \quad (1)$$

when the angles are expressed in radians and vertical and horizontal eye position are described in Helmholtz coordinates (Somani et al., 1998). When K equals 1.0, cyclodisparity is reduced to zero under open-loop conditions (i.e. without using feedback from cyclodisparity).

Binocular torsional alignment of the horizontal retinal meridians is maintained at near viewing distances with incyclovergence in upward gaze and excyclovergence in downward gaze compared to the torsion pre-dicted by Listing's law. In Fick coordinates, incyclovergence forms an 'A' pattern between the vertical meridi-

* Corresponding author. Fax: +1-510-643-5109.
E-mail address: schor@socrates.berkeley.edu (C.M. Schor).

0042-6989/01/$ - see front matter
PII: S0042-6989(01)00149-3

ans of the retinas and excyclovergence forms a 'V' pattern. These changes in cyclovergence were originally described by Allen (1954) as a violation of Listing's law which states that eye orientation can be described with two degrees of freedom in terms of eye rotations from primary position about axes that lie in a single plane (Listing's plane). Primary position is in a direction that is orthogonal to Listing's plane. Recently the cyclovergence observed with gaze elevation during convergence has been reinterpreted as resulting from a divergence of Listing's planes (i.e. temporal rotation of each plane) and their corresponding primary positions in proportion to the angle of convergence (Mok et al., 1992; Van Rijn & Van den Berg, 1993; Minken & van Gisbergen, 1994). In this interpretation, Listing's law has not been violated because the cyclotorsion associated with eye elevation during convergence can still be described by axes of rotation lying in two planes, one for each eye. Another consequence is that cyclodisparity between images formed on the horizontal meridians of the two retinas does not change with gaze elevation during symmetrical convergence. The change in orientation of Listing's planes with convergence has been called the binocular extension of Listing's law, or L2 (Van Rijn & Van den Berg, 1993; Tweed, 1997). The constant K (Eq. (1)) describes the ratio of the yaw-tilt difference or divergence of Listing's planes over the change in convergence. During symmetrical convergence, if the primary positions were to diverge by the amount of convergence, then $K = 1.0$, and the resulting torsion would maintain alignment of the horizontal retinal meridians during symmetrical convergence and thereby maintain zero cyclodisparity. Targets in the visual plane that were nearer or farther from the point of fixation would be imaged with pure horizontal disparities. This would simplify the binocular matching problem of determining which retinal image points in the two eyes correspond to a single target in space by giving a preference to matches of images formed on epipolar retinal meridians (Marr & Poggio, 1979; Van Ee & Schor, 1999).

Do binocular vergence couplings exhibit plasticity? Previously, plasticity has been demonstrated for two of the three dimensions of vergence. The gain of the accommodative-vergence coupling can be increased or decreased by adapting appropriately to mismatches between the stimulus to accommodation and convergence (Judge & Miles, 1985; Eadie, Gray, Carlin, & Mon-Williams, 2000). Vertical vergence can be adapted to magnifiers placed before one eye to either increase or decrease with changes in tertiary gaze (McCandless & Schor, 1997; Schor & McCandless, 1997) and to vary with convergence (Schor & McCandless, 1995a,b). The current study demonstrates an adaptation of convergence-dependent changes in cyclovergence, as quantified by K and described by Listing's extended law, that normally bring the horizontal meridians of the retinas into close alignment with the visual plane during vertical gaze in symmetrical convergence. The following experiments demonstrate that we can either exaggerate or reduce the normal convergence-dependent variations of cyclovergence with vertical gaze by adapting to appropriate patterns of cyclodisparity stimuli. Changes of cyclovergence with vertical gaze and convergence are summarized as changes in the angle made by the intersection of the primary positions of the right and left eyes. We have used a biomechanics model of the oculomotor system to explore how these adaptations might be implemented.

2. Methods

2.1. Apparatus

Three-dimensional eye position was recorded objectively using video-oculography, or VOG (SMI, Germany). The resolution of the system is better than 0.20° vertical, 0.01° horizontal and 0.025° torsional (Clarke, Teiwes, & Scherer, 1991; Clarke, 1994). Resolution is also estimated by the mean standard deviations of torsion from Listing's plane that we report are equal to or less than 0.5° for measures taken over a 20° range of vertical and horizontal eye positions. The SMI system uses infrared CCD cameras to image the two eyes, and in software it calculates eye position in three dimensions (horizontal, vertical and torsional). The two cameras, infrared-reflecting mirrors, and LEDs of the SMI system were mounted in a custom-made rigid aluminum frame that allowed reproducible positioning of the subject relative to the camera system by using a mouth-bite and head restraint apparatus. Prior to the experiment, the mirrors and cameras were adjusted so that their optical axes were parallel to the straight-ahead reference position (a direction that is orthogonal to a fronto-parallel projection screen). Optical alignment was calibrated with a mechanical gimbaled eye with the axes nested in Fick coordinates (earth-fixed vertical, eye-fixed horizontal axis). The mechanical eye was positioned in the apparatus so that its primary position coincided with the straight-ahead reference direction. The angles between the infrared-reflecting mirrors were adjusted to obtain zero torsion in Fick coordinates (for an explanation of coordinate systems, see Schor et al., 1994) with secondary and tertiary movements of the mechanical eye from primary gaze. The SMI system measures eye position in Fick coordinates. We defined zero torsion and zero horizontal and vertical eye position as the orientation of both lines of sight while fixating the straight-ahead distant target. Straight ahead was defined when the inter-auditory meatus, eye center and central fixation target were coplanar and parallel to the floor. The

subject fixated targets on a tangent screen, the center of which was 119 cm away, with anaglyphic targets separated by the interpupillary distance. In the straight-ahead position, this target stimulated parallel eye alignment and an accommodative stimulus of 0.84*D*.

Camera images of the two eyes were captured with a frame grabber at a rate of 60 Hz. Torsional change was represented as an angular difference between iris features taken on successive frames and a reference segment (Clarke et al., 1991). In this technique, a luminance-iris signature (reference segment) was obtained with a 90° arc taken from the lower region of the iris. The reference segment was obtained from each of the two irises at the beginning of each experimental session. This reference segment, obtained when the eye was aimed straight ahead, was cross-correlated with segments obtained in successive frames from the same iris location. The shift of the peak of the cross-correlation between the reference and subsequent segments was taken as the torsional position of the eye. The same reference segment was also used after 2 h of training, allowing us to describe differences between pre-trained and post-trained torsion, both of which were measured relative to torsion in the straight-ahead position at the beginning of the experiment. All iris segments obtained during the experiment were corrected in real time for the geometric distortion of an arc that occurs in eccentric gaze (Moore, Haslwanter, Curthoys, & Smith, 1996). Additionally, because torsion itself is variable (Van Rijn et al., 1994), calibration data were collected for 5 s with the subject looking straight ahead and averaged offline. The average for each eye was then subtracted from all subsequent measures as our best estimate of the true torsion associated with straight-ahead viewing. Horizontal and vertical eye positions were calculated from measures of the pupil center. During calibration, subjects fixated targets subtending zero vergence at five horizontal and five vertical positions over a range of $\pm 10°$ along the vertical and horizontal meridians. Measurements of the three dimensions of eye position were presented in a real-time display and saved to disk for off-line analysis.

2.2. Stimuli and training

We investigated plasticity of the cross-coupling between cyclovergence and convergence with vertical gaze in response to computer generated torsional disparities that varied with vertical eye position and convergence angle. Two adaptation procedures were conducted, one that reversed the normal pattern of convergence-dependent cyclodisparity variations with vertical gaze and another that exaggerated the pattern. The two patterns of cyclodisparity are shown schematically in Fig. 1a, b. In the reversed condition (Fig. 1a), cyclodisparities were presented in the midsagittal plane with incyclodisparity in upward gaze and excyclodisparity in downward gaze for far fixation and the opposite pattern (excyclodisparity in up gaze and incyclodisparity in down gaze) was presented for 10° convergence in near fixation. Fig. 1b is a schematic representation of the exaggerated condition in which the pattern of cyclodisparities was opposite to that in the reversed condition. Each cyclodisparity was 5° and vertical eccentricity was $\pm$ 10°. The disparate fusion patterns shown in Fig. 1c consisted of a 53° rectangular grid with three concentric circles superimposed on its center. During a 2-h training period, subjects viewed the four torsional disparity stimuli one at a time and targets were selected by pressing a button on a game pad. Fixations averaged approximately 10 s at each target location. The actual retinal image cyclodisparities subtended by these targets depended in part on the individual subject's baseline cyclophoria. Pre-trained cyclophorias varied little with vertical gaze. Across subjects, pre-trained cyclophorias ranged from 0.12° to 2.2° over the 20° range of vertical eye positions. These baseline cyclophorias may have increased or decreased the retinal disparity of the adapting stimulus by at most 20%. In no case did the cyclophoria change the pattern of retinal torsional disparities subtended by the training stimulus from reversed to exaggerated, or from exaggerated to reversed.

Each of the four subjects was trained and tested during two sessions that were separated by at least 2 days of normal binocular vision to avoid the possibility of residual aftereffects from the first session. In one training session the subjects went through the reversed condition and in the other the exaggerated condition. The three authors and one naive observer (MH) served as subjects. All four subjects had normal eye alignment and stereopsis. The subjects gave their written consent to participate in these experiments.

Anaglyphic (red–green) stimuli were displayed with an LCD rear-projection system. Targets were viewed through a red filter before the right eye and a green filter before the left eye so that each eye saw only one target. Because the training targets were projected onto a tangent screen and rotated about the axes orthogonal to the screen and not the subject's line of sight, there was a slight nonuniformity of the cyclodisparities although this asymmetry was not apparent to the subjects.The horizontal separation between left and right eye targets was controlled to stimulate 0° of convergence (parallel visual axes) and 10° of convergence, which is equivalent to a viewing distance of approximately 34 cm. The normal accommodative stimuli associated with these convergence angles are 0 and 2.9 diopters, respectively. The rear-projection screen was located 1.19 m from the subject and presented a 0.84*D* stimulus to accommodation for both the far and near convergence stimulus. Subjects reported that they could

fuse and clear both combinations of accommodative and convergence stimuli. Prior studies of Listing's extended law have used prisms to stimulate convergence and these stimuli also produce a mismatch between stimuli for accommodation and convergence (Mikhael, Nicolle, & Vilis, 1995; Somani et al., 1998).

Open-loop cyclovergence (cyclophoria) responses to a non-fusable stimulus were measured objectively at the beginning and end of the 2 hour training period at 25 target locations in a 5×5 square grid configuration at points separated vertically and horizontally by 5°. Stimuli were stepped vertically every 5 s through the five targets from up to down gaze along each vertical column, starting with the center column, then to the left column and progressing to the right column. The open-loop stimuli were presented at the two test distances (0 and 10° convergence). We also measured the open-loop cyclophoria along the center column presented with a horizontal disparity corresponding to 15° of convergence.

The open-loop fixation target was a 2° diameter red circle seen by the right eye surrounded by two 2° green horizontal lines seen by the left eye. This fixation target provided an open-loop stimulus for both vertical and torsional vergence. Subjects controlled their horizontal vergence volitionally while they fixated the 25 points at either the simulated near or far viewing distances. Vertical phoria was allowed to vary because extraocular muscles used for vertical movements also may induce torsion at certain version angles (Enright, 1980; Mikhael et al., 1995) and we were concerned that the effort used to fuse targets vertically might affect measured open-loop torsion. Differences between post-adapted and pre-adapted measures of cyclophoria were used to quantify convergence-dependent changes in the primary position vergence angles.

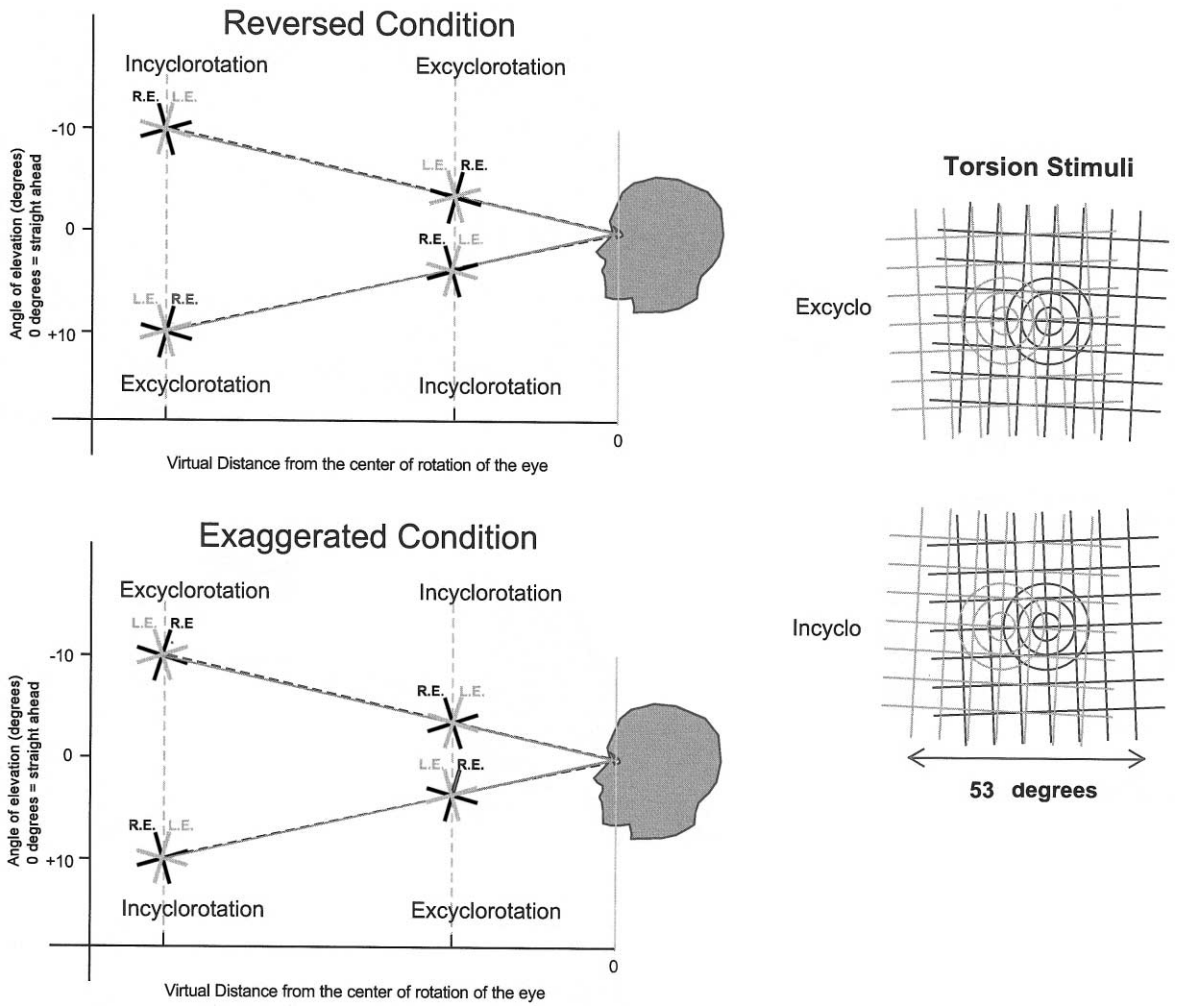

Fig. 1. The patterns of torsional disparity used in the exaggerated (lower left) and reversed (upper left) conditions are shown schematically. Ten degree changes in cyclodisparity are presented at a far and a 10° near convergence distance. At one distance incyclodisparity is presented in upward gaze and excyclodisparity in downward gaze and the reverse pattern is presented at the other convergence distance. The fusion pattern consisted of a 53° rectangular grid with three concentric circles superimposed on its center.

2.3. Data analysis

The results are described in two ways, (1) as adapted changes in primary position or orientation of Listing's plane measured at a far and near convergence angle and (2) as adapted changes in cyclophoria with specific combinations of convergence and vertical eye position. For the Listing's plane analysis, three-dimensional measures of eye position were converted from Fick coordinates to rotation vectors relative to the straight-ahead reference position (Haustein, 1989; Haslwanter, 1995). Rotations are about three head-fixed orthogonal axes pointing forward, leftward and upward. Following the right-hand rule, positive rotations about these axes produce clockwise, downward and leftward rotations. Measures of rotation vectors at the 25 test points were fit by a least squares analysis to a plane (displacement plane), and the parameters describing the plane were used to quantify the change of torsion with vertical and horizontal eye rotation. The thickness of the plane was quantified as the standard deviation in degrees of torsional eye positions around the plane. The yaw slope of the displacement plane describes changes of torsion with vertical eye rotation and the pitch slope of the displacement plane describes change of torsion with horizontal eye rotation relative to the straight-ahead direction. Primary position is defined as the normal to Listing's plane (for explanation see Tweed, 1997). The primary position of gaze is found by doubling the displacement plane pitch and yaw tilt angles according to the half angle rule (Tweed & Vilis, 1990). Changes in horizontal (yaw) and vertical (pitch) components of primary position were used to quantify the changes produced by the two training procedures.

We compared primary positions derived from pre- and post-adapted conditions and observed how they changed with convergence. We quantified the difference between the right and left eyes' primary positions (right–left) for both yaw and pitch. The yaw tilt difference (YTD) describes the horizontal vergence angle between primary positions and the pitch tilt difference (PTD) describes the vertical skew between the primary positions (Bruno & Van den Berg, 1997). Following the right hand rule, a divergence of primary positions is a positive YTD, and a right/left vertical skew (right eye higher) is a negative PTD. The gain of the change in YTD with convergence (K) equals the YTD (near–far) divided by the change of convergence (near–far).

Our three-dimensional measures of eye position were in Fick coordinates. The Fick system needs to be rotated about its optical axis by a correction factor called false torsion to describe radially symmetric rotation of the eyes that obey Listing's law. In our cyclophoria analysis, the torsional component of the rotation vector (given in degrees) of each eye's position was approximated by subtracting the false torsion (F) from the measured Fick torsion (T) (Porrill, Ivins, & Frisby, 1999).

$$F = 2\tan^{-1}(\tan(V/2) \times \tan(H/2)) \quad (2)$$

where V, H and T equal vertical and horizontal and torsional components of eye position given in degrees in Fick coordinates (Helmholtz, 1962). Our measure of cyclophoria (Cv) equalled the difference between the corrected open-loop measures of Fick torsion of the right (r) and left (l) eyes (r–l).

$$Cv = (T\mathrm{r} - F\mathrm{r}) - (T\mathrm{l} - F\mathrm{l}) \quad (3)$$

The cyclophoria analysis evaluated the spread of cyclovergence aftereffects from the trained zero horizontal version meridian to untrained horizontal directions of gaze.

Cyclophoria was plotted as a function of vertical eye position for each of the five tested horizontal gaze directions. Slopes of linear regression fits to the scatter plots yielded the change in cyclophoria in relation to vertical eye position (vertical-cyclophoria gradient) at a given horizontal gaze direction, and the intercept of the fit described the overall offset or cyclophoria bias. The slope of the regression in the example shown in Fig. 2 represents the vertical-cyclophoria gradient measured before and following training to excyclodisparity in up gaze and to incyclodisparity in down gaze. Differences between slopes for post-adapted and pre-adapted conditions (post–pre) were used to quantify the adapted change in the vertical-cyclophoria gradient (Δcyclophoria gradient). The gain of the adapted response equalled the ratio of Δcyclophoria gradient/stimulus gradient. The stimulus gradient equalled the change in cyclodisparity (degrees) per degree change in vertical position (10°/20° or 0.5). The same sign convention was used to describe the stimulus-disparity gradient and response-cyclophoria gradients. Positive gains indicate that the cyclophoria changed in the same direction as the training stimulus. The gains show how well subjects adapted cyclovergence at a given convergence angle. The gain of the adapted response was analyzed separately for each of the five horizontal gaze directions at both the far and near (10° convergence) trained distances and at a 15° untrained vergence angle in symmetrical convergence. In Section 3, the cyclophoria analysis illustrates the spread of aftereffects away from the trained direction and distances of gaze. In Section 4, the displacement plane analysis illustrates adapted changes in the gain (K) of Listing's extended law.

3. Results: cyclophoria analysis

3.1. Does open-loop cyclovergence adapt to a cyclodisparity gradient stimulus?

The reversed and exaggerated training conditions

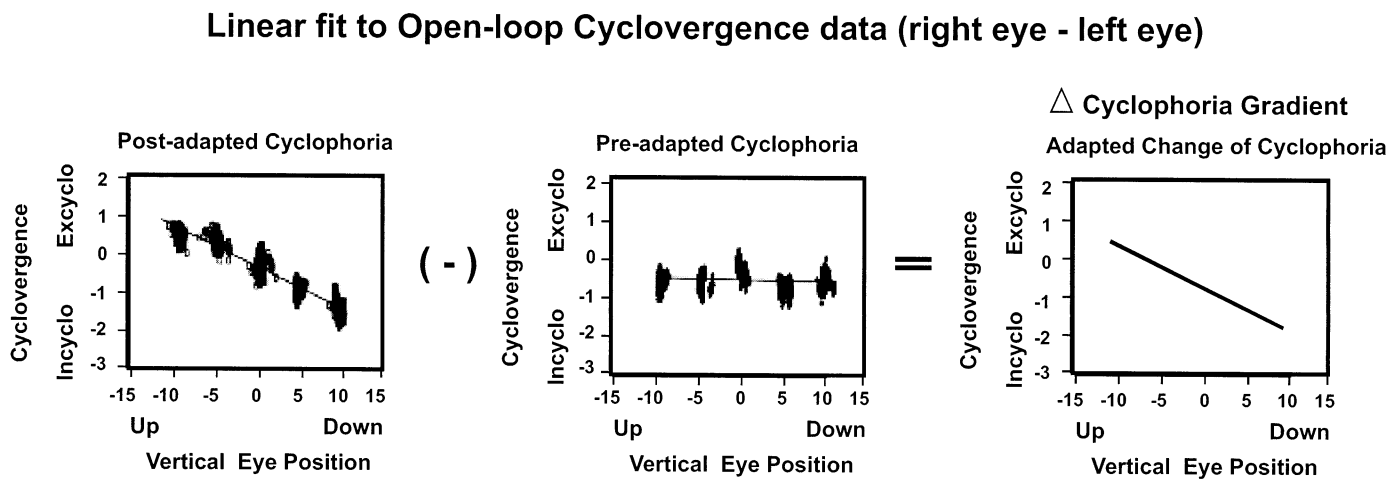

Fig. 2. Linear regression analysis of adapted changes in vertical cyclophoria gradients. Cyclophoria equals right–left eye torsion.

were designed to decrease or increase the normal changes in cyclovergence that occur with convergence and vertical gaze. Fig. 2 is an example of the change in vertical-cyclophoria gradient at the far-vergence distance that resulted from training with the exaggerated condition. Prior to training, the cyclophoria varied little with vertical eye position at the far convergence distance. After training, cyclophoria varied with vertical eye position from excyclo in up gaze to incyclo in down gaze.

Fig. 3 shows the gain of adapted changes in the vertical-cyclophoria gradient, measured along the midsagittal plane (symmetrical convergence) at the two trained convergence distances of 0° and 10° and at an untrained convergence distance of 15°. Gains were calculated from post–pre measures of vertical-cyclophoria gradient/stimulus gradient. Positive and negative gains indicate whether the adapted cyclophoria was in the same or the opposite direction as the disparity of the training stimulus. Vertical-cyclophoria gradients that changed in the same direction as the training stimulus are represented by positive gains, and cyclophoria gradients that changed in the opposite direction as the stimulus gradient have negative gains. Inspection of Fig. 3 illustrates that the largest changes in cyclophoria for the reversed condition occurred at the near-convergence test distance (striped bars) (ranging from 8% to 24% of the stimulus-disparity gradient), whereas the largest changes in cyclophoria for the exaggerated condition occurred at the far test distance (black bars) (ranging from 12% to 34% of the stimulus-disparity gradient). One exception is subject JM whose gains increased at both vergence distances in the reversed condition. The significance level of the gains was tested using an ANCOVA (analysis of covariance) that compared pre- and post-regression slopes for individual subjects. All subjects' pre and post measures were significantly different at the 95% level of confidence. We also quantified the spread of the aftereffect trained at 10° of convergence to an untrained 15° of symmetrical convergence. The Δvertical-cyclophoria response gradients for 15° were scaled by the same stimulus gradient (0.5) so that the magnitude of changes in cyclophoria at the two near distances could be compared. The gains shown in Fig. 3 for the two near convergence distances

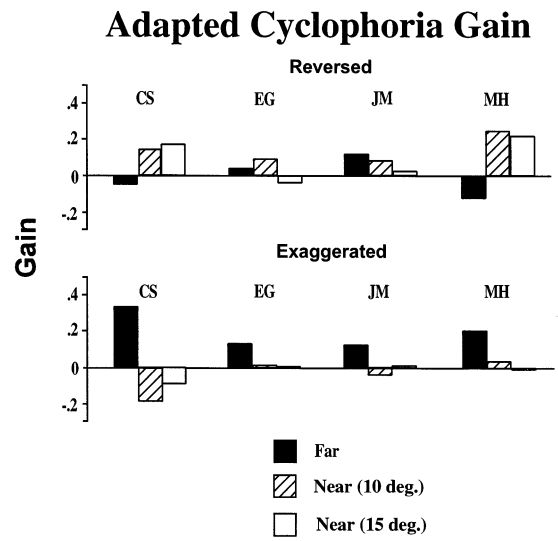

Fig. 3. Gain of adapted changes of vertical-cyclophoria gradients (post-pre) measured during symmetrical convergence in the midsaggital plane at a far and two near test distances (10° and 15° of convergence). Gains equal the slopes shown in Table 1 divided by the cyclodisparity stimulus gradient (0.5). Positive values signify changes in cyclophoria that reduced the retinal image disparity subtended by the training stimuli shown in Fig. 1. The largest changes occurred at the far test distance following training to the exaggerated condition and at the near test distances following adaptation to the reversed condition.

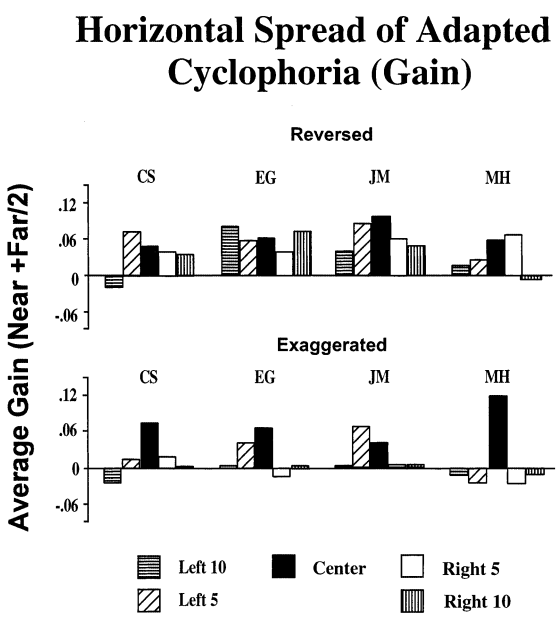

Fig. 4. Spread of aftereffects from the central horizontal trained direction of gaze to untrained horizontal gaze directions of 5° and 10°. Adapted gain change (post-pre), is averaged for the far and 10° convergence test distances, (far + near)/2. Positive values illustrate changes in cyclophoria that conformed to the disparity patterns presented at the two stimulus distances. Adapted changes in averaged gain for the reversed condition spread from the central trained direction to untrained horizontal gaze directions of 5 and 10°. In contrast, the adapted changes in averaged gain for the exaggerated condition were restricted to the central five-degree range of horizontal eye positions.

illustrates that the changes in cyclophoria at the trained near vergence distance carry over to a nearer untrained vergence distance.

The intercept of the linear regression analysis (not shown) revealed a fairly consistent cyclophoria bias following training. In all but one subject in one condition (EG exaggerated), the post-training bias increased in the incyclophoria direction. The intercept values ranged from 1° to 4° and they were independent of whether the gain change shown in Fig. 3 was positive or negative. The combination of incyclophoria bias with the gain changes shown in Fig. 3 produced the largest increases of incyclophoria in the lower gaze direction. This corresponds to the near convergence distance in the reversed condition and the far convergence distance in the exaggerated condition.

3.2. Can the coupling of cyclovergence with convergence be changed by training, and do these changes spread from trained to untrained horizontal directions of gaze?

The average of the gain for the near and far test distances, (far + near)/2, represents how well cyclophoria adapted to the stimulus training condition as a whole. If adaptation of cyclovergence was not coupled with convergence and cyclophoria only adapted to the stimulus at one distance, then the same changes in cyclophoria would occur at both the near and far test distances. The gain that quantified this change would be positive for one distance and negative for the other distance, and the average gain would be zero. If adaptation of cyclovergence were coupled with convergence and cyclophoria adapted to conform to disparities at both the far and near distances, then the gain would be positive for both distances, and the average would be positive. Adapted changes in coupling between cyclovergence and convergence could also result from unequal changes of cyclophoria in the same direction at both test distances. For example there could be a combination of a positive gain at one distance and a smaller negative gain at the other distance. Fig. 4 tests for coupling of convergence with cyclovergence adaptation by averaging the adaptation gain at the far vergence distance with the adaptation gain of the 10° convergence test distance. Black bars represent the average gain of the trained central fixation direction and the textured and open bars represent the average gain at untrained horizontal gaze eccentricities of 5° and 10° to the left and right of center. The black bars illustrate that all subjects had positive average gains for both disparity-training conditions that ranged from 5% to 12% of the combined near and far cyclodisparity stimulus gradients. Textured and open bars illustrate that spread of the trained aftereffect to untrained directions depended on the training condition. A moderate spread of the trained aftereffect, over a 20° range of horizontal eye positions, was observed in the reversed condition. All four subjects had a narrower spread of aftereffects for the exaggerated condition. In this condition, their aftereffects were restricted to a central 5° range of horizontal eye positions. One of the authors (C.S.) made perceptual observations during the exaggerated training period that were consistent with the non-uniform narrow spread of the aftereffect to untrained directions of gaze. He noticed that the grid pattern appeared fused and horizontal while fixating along the center horizontal direction (symmetrical convergence), but when he diverted his gaze by 10° to the right or left of the center, the grid appeared to have a large torsional disparity. When he shifted his gaze back to the center, the pattern immediately appeared fused and horizontal again.

4. Results: Listing's plane analysis

4.1. Does Listing's extended law exhibit plasticity?

Fig. 5 illustrates an example of pre-adapted front and top-down views of displacement planes for a straight-

ahead reference direction of the right and left eye. Displacement planes were obtained from VOG measures of three-dimensional recordings of angular eye position represented in degrees as rotation vectors with a straight-ahead reference direction (Haustein, 1989; Haslwanter, 1995). Three-dimensional measurements of binocular eye position were taken with the two eyes viewing an open-loop stimulus presented in 25 locations at the far test distance. The measures were fit by least squared analysis to a plane. The fit parameters of the calculated planes were used to describe the yaw, pitch and offset of the resulting displacement planes relative to a straight-ahead reference direction. The yaw tilt corresponds to the slope of the horizontal axis of the plane, the pitch tilt to the vertical axis slope and the offset to the nasal-occipital shift of the planes. The goodness of fit described the thickness of the plane and it was quantified as the standard deviation of torsional eye positions (degrees). Standard deviations ranged from ± 0.27 to ± 0.73 and the mean value of the standard deviation for all test conditions was equal to or less than $\pm 0.5°$ which is comparable to the plane thickness measured with search coils (Bruno & Van den Berg 1997). The differences between thickness of post- and pre-adapted planes for each test distance and adaptation condition were evaluated by a paired samples t-test and found not to be significant ($P < 0.05$).

The yaw and pitch orientations of displacement planes were doubled to obtain estimates of the orientation of Listing's plane. The orientations of the Listing's planes were described by the yaw and pitch angles of the normal to the plane (primary positions). The purpose of this analysis was to quantify differences in the primary positions of the two eyes (right–left) and their changes following adaptation. Positive yaw-tilt differences (YTD) between primary positions represent an increase in excyclovergence in down gaze and a divergence of primary positions of the two eyes. Positive pitch-tilt differences (PTD) represent an increase of excyclovergence in left gaze and a left/right skew (left-hyper) deviation between primary positions. Results following training that conformed to the torsional disparity pattern presented in the reversed training condition would be expected to have an increased positive or decreased negative YTD at the far distance and a decreased positive or increased negative YTD at the near convergence distance. Results following training that conformed to the torsional disparity pattern presented in the exaggerated condition would have the opposite pattern of changes of YTD of primary position. Neither training condi-

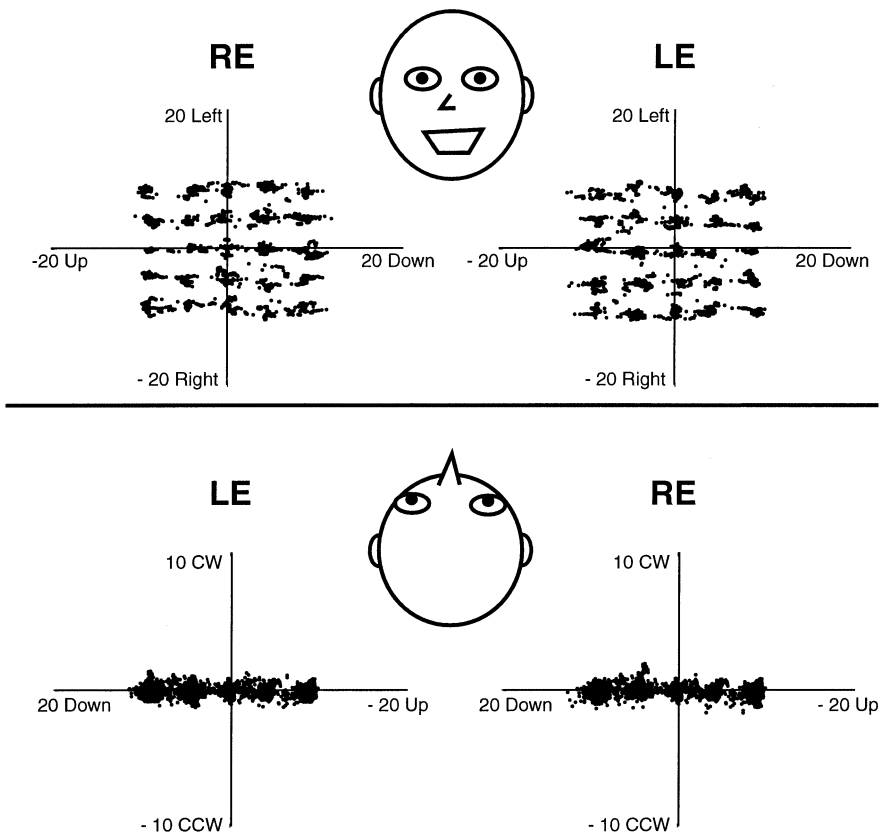

Fig. 5. An example of pre-adapted front and top-down views of displacement planes for a straight-ahead reference direction of the right and left eye. Measurements were taken with the two eyes viewing an open-loop stimulus presented in 25 locations at the far test distance.

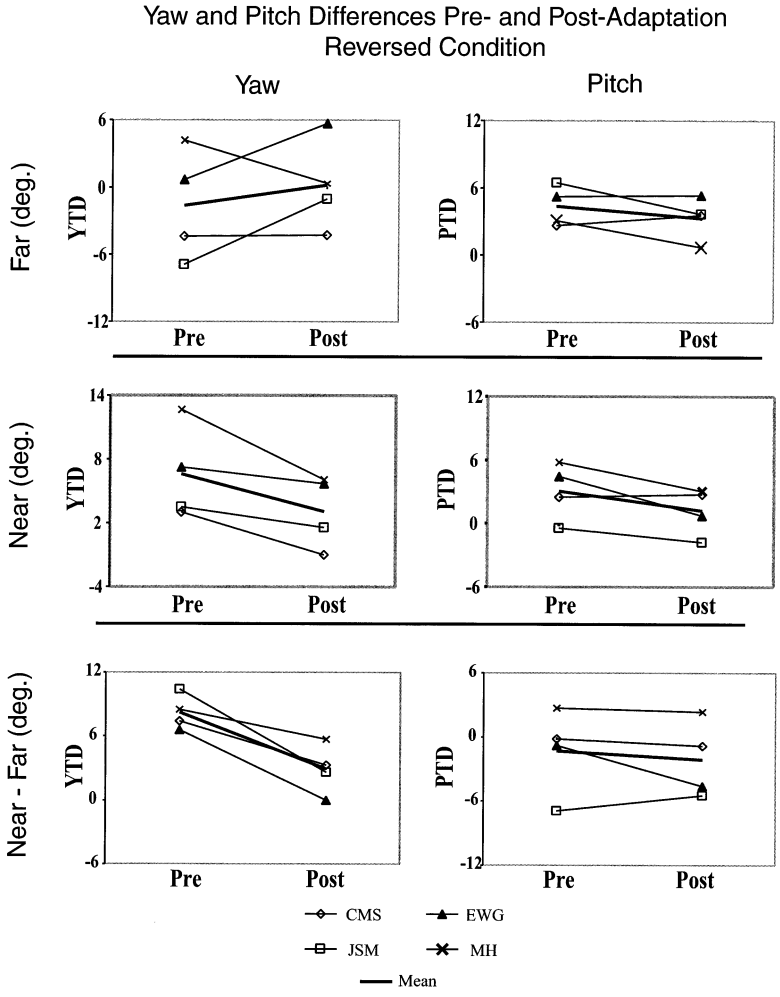

Fig. 6. Reversed condition: thin lines connect pre and post measures of the YTD (left column) and PTD (right column) between right and left eye primary positions for individual subjects and the heavy line represents the mean. Results for the far (0° convergence) and 10° convergence distance are plotted separately, and a third panel illustrates the difference between far and near measures of post-pre YTD and PTD. Negligible changes occurred in PTD. YTD changed in opposite directions at the two test distances and the change was larger at the near (10°) convergence distance.

tion would be expected to produce any consistent changes in PTD.

Results for the reversed and exaggerated conditions are shown in Figs. 6 and 7, respectively. They illustrate results for individual subjects and the mean for all subjects combined. Thin lines connect pre and post measures of the YTD and PTD of primary positions for individual subjects and the heavy line represents the mean. Results for the far (0° convergence) and near (10° convergence) distances are plotted separately, and a third panel illustrates the difference between far and near measures of post-pre YTD and PTD. Note that the data for the two training conditions were collected on separate days and that the same optical alignment, head position, reference images and calibration were used for pre- and post-tests on a given day. Although the two pre-measures of yaw and pitch tilt differences for the reversed and exaggerated condition were measured on separate days, they were within 2.5° of one another. Pre-adapted YTD means for the far reversed and the far exaggerated condition were $-1.6°$ and 0.65° and means for the far pre-adapted PTD were 4.4° and 1.83°, respectively. Pre-adapted YTD means for the near reversed and the near exaggerated conditions were 6.6° and 8.8°, and means for the near pre-adapted PTD were 3.1° and 1.8°, respectively. These changes are well within the day-to-day variations of primary position reported with search coil measures (Melis, Cruysberg, & van Gisbergen, 1996)

The adapted changes of YTD shown in Fig. 6 for the reversed condition follow the predicted trends. YTD for the reversed condition became less negative or more positive for three subjects at the far test distance and less positive or more negative for all four subjects at the near convergence distance. Post-pre changes in far YTD ranged from 5.8° to $-3.8°$ for individual subjects with a mean change of 1.8°. Post-pre changes in near YTD ranged from $-1.5°$ to $-6.6°$ for individual

subjects with a mean change of −3.5°. Post-pre changes in YTD for the exaggerated condition (Fig. 7) were negative or less positive for all subjects at both the far and near convergence test distance, however they were larger at the far than near convergence distance which is consistent with the predicted trend. Post-pre changes in far YTD ranged from −3° to −14° for individual subjects with a mean change of −7.5°. Post-pre changes in near YTD ranged from −0.6° to −10° for the individual subjects with a mean change of −5.3°. The changes in PTD were much smaller than YTD for all conditions, averaging less than 2°.

The bottom panels of Figs. 6 and 7 plot the difference between far and near measures of post-pre YTD and PTD. In both the reversed and exaggerated conditions, prior to training, the near YTD was more positive than the far YTD, demonstrating a divergence of Listing's planes with convergence as predicted by the binocular extension of Listing's law. Following training, the difference became smaller for the reversed condition and larger for the exaggerated condition. Differences between near and far PTD were negligible before training and changed idiosyncratically by small amounts following training on average.

The coupling between convergence and the YTD between primary positions of the two eyes is quantified by K in Table 1 as the change in YTD with convergence angle.

$$K = (\text{near YTD} - \text{far YTD})/\Delta\text{convergence} \quad (4)$$

Table 1 compares the pre-adapted with the post-adapted measures of K for the reversed and exaggerated conditions for individual subjects and their average. These ratios describe the changes in yaw angle between primary positions per degree of convergence. The pre-trained values of K range from 0.66 to 0.85 with a mean of 0.82, illustrating that when the eyes converge, Listing's planes diverge. These values are in close agree-

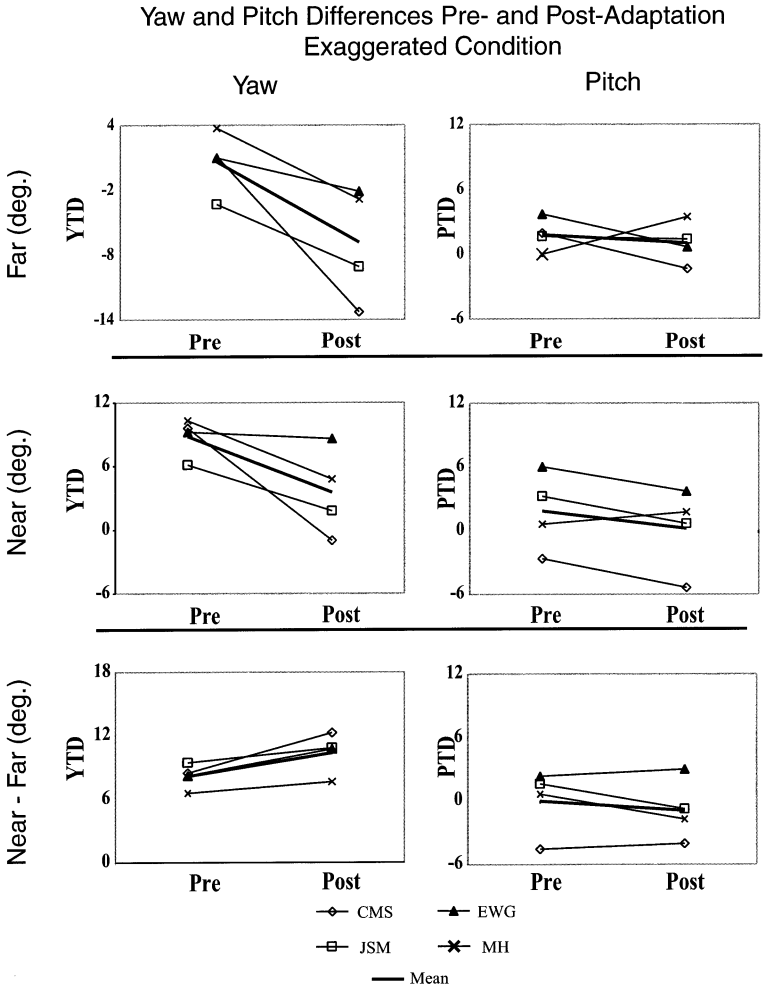

Fig. 7. Exaggerated condition: thin lines connect pre and post measures of the YTD (left column) and PTD (right column) between right and left eye primary positions for individual subjects and the heavy line represents the mean. Results for the far (0° convergence) and near (10° convergence) distance are plotted separately, and a third panel illustrates the difference between far and near measures of post-pre YTD and PTD. Negligible changes occurred in PTD. Larger negative changes in YTD occurred at the far than near test distance.

Table 1
Cross-link gains (K) between convergence and the yaw tilt difference (YTD) are derived from pre and post adapted measures of Listing's plane where K = change in YTD (near–far)/change in convergence distance

	Subject K-value				
	CMS	JSM	EWG	MH	Average
Reversed condition					
Pre	0.74	1.04	0.66	0.85	0.82
Post	0.33	0.26	0.00	0.57	0.29
Exaggerated condition					
Pre	0.84	0.94	0.82	0.66	0.82
Post	1.23	1.09	1.07	0.76	1.04

When $K = 1$, coupling between convergence, vertical gaze, and cyclovergence maintains a constant alignment or cyclodisparity between the horizontal retinal meridians with gaze elevation at all fixation distances. Following adaptation the average value of K decreased from 0.82 to 0.29 for the reversed condition and it increased from 0.82 to 1.04 for the exaggerated condition. On average, incyclovergence bias for the post condition increased by 0.9° for both near and far test distances

ment with those derived by prior studies (Mok et al., 1992; Minken & van Gisbergen 1994; Mikhael et al., 1995; Somani et al., 1998).

Values of K unequal to 1.0 indicate that the cyclophoria between horizontal retinal meridians is changing with convergence distance and gaze elevation, and a ratio of zero indicates that YTD between Listing's planes is the same at near and far convergence distances. Divergence of Listings planes during convergence was reduced by the reversed condition and increased slightly by the exaggerated condition. Prior to training, K averaged 0.82. The post-trained values for the reversed condition range from 0.0 to 0.57 with a mean of 0.29, and the post-trained values for the exaggerated condition range from 0.76 to 1.23 with a mean of 1.04. These results illustrate that the systematic changes in cyclovergence with vertical gaze that are linked to the amount of convergence are not rigid and that they can be modified with experience.

As in the cyclophoria analysis, translation of the adapted displacement planes along the torsion axis revealed a consistent incyclovergence bias between the right and left eye plane intercepts. In 14 of the 16 measures of right-left plane intercepts, the post measures were less positive or more negative than the pre measures, indicating a relative incyclovergence between the two planes (constant positive translation along the torsion axis in the left eye plane and negative translation in the right eyes' plane). The average increase in incyclovergence offset following training for all test conditions was 0.95°. These results are consistent with the cyclophoria offsets computed from intercepts of the regression analysis of cyclophoria and vertical gaze.

5. Discussion

5.1. Summary

Our adaptation procedure demonstrates that the coupling between cyclovergence, convergence and vertical gaze, known as the binocular extension of Listing's law, can be modified in response to patterns of cyclodisparity that vary with horizontal convergence and eye elevation. The modification is demonstrated in our analysis by changes in cyclophoria (open-loop cyclovergence) at the far and near convergence distances after adapting to patterns of cyclodisparity stimuli that either exaggerated or reversed the normal cyclovergence coupling with vertical gaze. The average gain of open-loop cyclovergence aftereffects (post–pre) to near and far stimuli presented in the trained directions was 7.4% of the amount stimulated in the exaggerated condition and 6.8% in the reversed condition (Fig. 4). These percentages correspond to near-far changes in cyclophoria of approximately 1.5° at a vertical gaze-eccentricity of 10° from the straight-ahead position. At a given convergence distance, the percentages also corresponds to up-down changes in cyclophoria of approximately 1.5°. Cyclophoria aftereffects of both training conditions also spread from the trained 10° convergence distance to the non-trained 15° convergence distance (Fig. 3). However, the aftereffect at the 15° test distance did not increase proportionally with the increase of convergence, suggesting that the adapted coupling diminished at the non-trained convergence distance.

Three-dimensional measures of eye position were used to derive the orientations of Listing's plane at two convergence distances (0° and 10°). Both the reversed and exaggerated training conditions altered the yaw-tilt differences between primary positions of the right and left eyes by different amounts at the two convergence distances (Figs. 6 and 7). The ratio (K) of change in YTD with change of horizontal convergence describes the magnitude of the coupling between cyclovergence and convergence. K values equal to 1.0 would indicate that the coupling between convergence (C), vertical gaze (V) and cyclovergence (Cv) maintained a constant alignment or cyclodisparity between the horizontal retinal meridians during gaze elevation at all fixation distances. This prediction follows the relationship $K = Cv/(C*V/2)$, where all angles are expressed in radians and cyclovergence is described in Listing's coordinates (Somani et al., 1998). The average pre-adaptation ratio for our subjects was $K = 0.82$, which is similar to the average values found in prior studies (Mok et al., 1992; Minken & van Gisbergen 1994; Mikhael et al., 1995; Somani et al. 1998). The pre-adaptation measures of K varied between subjects over a 36% range. Similar variations have been reported previously by Hooge and van den Berg (2000). This range is surprising given our

demonstration of adaptive plasticity for Listing's extended law. Why does the binocular system not have a consistent value of K equal to 1.0 under natural conditions? Natural near stimuli are often small objects held in the hand. Perhaps, near objects seen under natural viewing conditions do not require perfect compensation because they are too small to stimulate perfect motor compensation for cyclodisparities. Cyclofusion is primarily sensory for small field sizes under 20° in diameter, and a motor component dominates cyclofusion with larger fields (Kertesz & Sullivan, 1978; Howard, Sun, & Shen, 1994). Larger and more consistent values of K might be found in natural conditions if cyclovergence were stimulated by larger near field sizes such as those used in the current study, rather than the small fields usually presented under most natural near viewing conditions.

The average ratio following adaptation to the reversed adaptation condition decreased to $K = 0.29$. The ratio was reduced to zero for one subject (EWG) when YTD between primary positions became equal at the far and 10° convergence distance. If the YTD between primary positions had diverged more at the near distance, the ratio would have become negative. In that case primary positions would have converged with horizontal convergence. On average, the exaggerated adaptation condition increased K by half as much as it was decreased in the reversed adaptation condition. In the exaggerated condition, K increased from 0.82 to 1.04 (an increase of 0.22) and in the reversed condition K decreased from 0.82 to 0.29 (a decrease of 0.53). Complete adaptation to the patterns of cyclodisparity would have produced ratios equal to $K = +10.6$ for the exaggerated condition and $K = -10.6$ for the reversed condition, however our largest aftereffect for any subject was only one-tenth this magnitude (see Table 1; subjects CMS, JSM and EWG, exaggerated condition). The smaller average change in K in the exaggerated than reversed condition is likely due to the difference in spread of cyclophoria aftereffects shown in Fig. 4 from trained to non-trained horizontal directions of gaze. In the exaggerated condition, aftereffects were seen mainly in the trained center direction while in the reversed condition they spread to non-trained horizontal gaze eccentricities of 5° and 10°. The regression analysis showed that the gain of the aftereffects to the exaggerated and reversed conditions were similar in the trained directions of gaze. In the displacement plane analysis however, all horizontal positions are included resulting in a smaller aftereffect for the exaggerated condition. The results of the exaggerated condition demonstrate that it is possible to selectively adapt the vertical-cyclophoria gradient in a specific horizontal direction of gaze.

The limited spread of aftereffects with lateral gaze in the exaggerated condition is surprising given our prior work on non-concomitant vertical phoria adaptation. Those studies found that non-concomitant vertical phoria aftereffects spread uniformly to untrained gaze directions and distances (Maxwell & Schor, 1994; McCandless, Schor, & Maxwell, 1996; Schor & McCandless, 1997). The cyclophoria aftereffects at untrained locations might become more uniform with longer periods of training, or if the disparity stimuli were presented in several horizontal gaze directions, i.e. with a more natural pattern of disparities over a longer period of time.

During training, subjects observed that incyclodisparities were easier to fuse than excyclodisparities while alternating fixation between the upper and lower targets. The incyclophoria offset was present at both near and far test distances with one exception (EWG's offset in the exaggerated condition was negligible). An incyclovergence offset between left and right eye displacement planes was also estimated from the right-left eye difference between intercepts of displacement planes. On average, this measure of incyclovergence bias increased by 0.9° for both near and far test distances. Even when cyclophoria adapts to a single torsional disparity, cyclophoria aftereffects are greater in the incyclo than excyclo direction (Maxwell, Graf, & Schor, 2001). Sullivan and Kertesz (1978) observed a similar bias with more rapid incyclovergence than excyclovergence movements in response to step changes in cyclodisparity although the amplitude differences in that study were negligible.

5.2. Central versus peripheral mechanisms

How might convergence-coupled modifications of cyclovergence be implemented? Cyclovergence could be adapted by an active central process that couples the innervation of the vertical recti and obliques with specific combinations of convergence and vertical versional eye position. In this model, cyclovergence would be determined by an equivalent look-up table for various combinations of convergence and vertical eye position. Alternatively, adaptation of cyclovergence could be mediated by a central process that couples the innervation of the vertical oculomotor muscles (recti and obliques) with convergence, without explicit regard to versional eye position. In the latter case, orbital mechanics would passively constrain cyclovergence to vary with direction of gaze. The plausibility of the latter hypothesis was tested by simulating the normal convergence-dependent variations of cyclovergence with a biomechanical model (Orbit™) by scaling the gain of vertical recti and obliques with convergence.

Orbit™ is a biomechanics model that simulates binocular eye position based upon the relationships of the six extraocular muscles, their tendons and supportive connective tissues including muscle sheaths or pul-

leys, innervation level and motor nucleus connection weights (innervation gain) according to equations given, in part, by Robinson (1975) and Miller and Robinson (1984). Orbit™ was designed to follow both Hering's and Listing's laws for distance viewing but currently does not automatically implement the binocular extension of Listing's law. Hering's law is simulated by finding the innervation to an assumed normal following eye that would produce the same gaze direction as that of the fixating eye. Orbit™ simulates binocular alignment when the two eyes are dissociated (i.e. vergence is open-loop), such that one eye fixates various target directions while the following eye is guided by Listing's and Hering's innervations. Parameters of either eye or both eyes may be modified and torsion is allowed to deviate from Listing's law in both the fixating and following eye.

5.3. Coupling cyclovergence and horizontal vergence

In Orbit™, we adjusted innervation levels to horizontal recti to simulate 20° of convergence and the innervation gain to vertical recti and/or obliques to simulate convergence dependent changes in ocular torsion that are consistent with an ideal K ratio approximating 1.0. The same value of K was achieved by decreasing the innervation gain for the obliques by 30% or the increasing the innervation gain for the vertical recti by 30% or a combination of 15% increased gain to vertical recti and 15% decreased gain to obliques. Any combination yielding a gain change of 30% produced equivalent results. Simulations were conducted for 15 combinations of vertical and horizontal eye positions over a 60° range with 30° horizontal increments (left, center and right vertical columns) and 15° vertical increments in each column, in a 3×5 rectangular grid configuration centered in the midsagittal plane. Simulations of three-dimensional eye positions were transformed from Fick coordinates to rotation vectors relative to the straight-ahead reference position (Haustein, 1989; Haslwanter, 1995). Rotation vectors were fit with a linear regression to a plane and the top-down view of the displacement planes for the left and right eye are plotted in Fig. 8 to illustrate changes in torsion along the yaw axis when the eyes converge 20°. The primary position of gaze is calculated by doubling the displacement plane yaw and pitch angles.

Fig. 8 illustrates a top-down view of displacement planes for a straight-ahead reference direction of the right and left eye while the eyes converged 20°. Planes were derived from Orbit™ simulations of three-dimensional eye position with modified gains described above, during 20° of convergence. Rotation vectors of simulated eye positions in all three vertical test columns are combined into a single plot. Primary positions of the two eyes that correspond to these displacement planes each abducted 9.12°. The difference in the primary positions of the two eyes was 18.25°, which corresponds to a K value of 0.925 for the simulated 20° of convergence. Pitch of the planes was near zero. Orbit simulations (not shown) with normal gain values and 0° of convergence (far fixation) resulted in displacement planes that were parallel to one another in the fronto-parallel plane such that primary position was straight ahead during far fixation. The simulation demonstrates that simple convergence-related gain changes of the vertical ocular muscles are sufficient to transform the innervation pattern appropriate for torsion at far view-

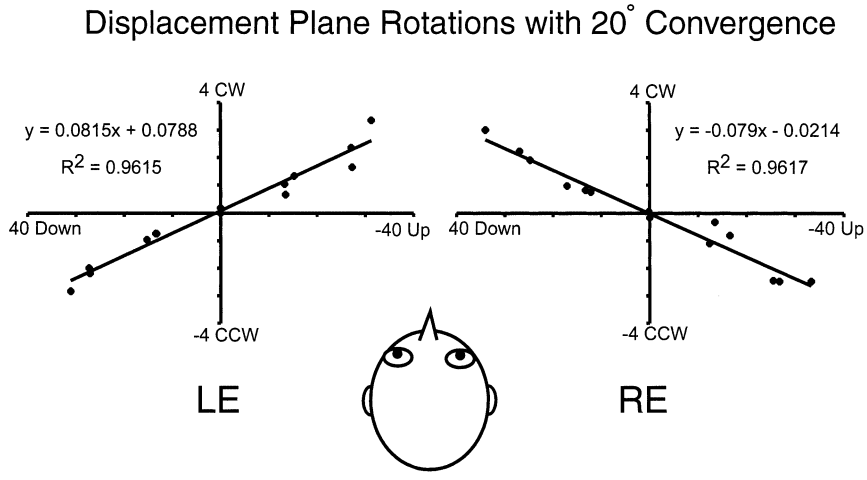

Fig. 8. A top-down view of simulated displacement planes for a straight-ahead reference direction are shown the right and left eye during 20° of convergence. Planes were derived from Orbit™ simulations of three-dimensional eye position with modified gains of the obliques and vertical recti. The Orbit™ simulations are for a 15% decreased gain of the obliques and 15% increased gain of the vertical recti. Torsion, plotted in degrees, is simulated for vertical and horizontal changes in eye positions over a 60° horizontal and vertical range. Fifteen test points ranged from the near central fixation point in 30° horizontal increments and 15° vertical increments in a 3×5 rectangular matrix. YTD of the two displacement planes equals 9°, which corresponds to a YTD between primary positions of 18° and a K value equal to 0.9.

ing distances into ones consistent with Listing's extended law at near viewing distances. These gain changes can be decreased or increased to describe the empirical measures of adaptive plasticity of K observed in current study. The empirical reductions of K that resulted from the reversed adaptation condition could be modeled by reducing the gain changes in our simulation toward standard values for Orbit. Similarly, the increases in K that resulted from the exaggerated adaptation condition could be modeled by increasing the gain changes for Orbit that are described by the simulation shown in Fig. 8.

Other simulations (not shown) indicate that reduced innervation of the superior oblique alone is insufficient to account for the convergence induced changes in torsion observed with vertical gaze (Allen & Carter, 1967). As demonstrated in Fig. 8, in addition to reduced innervation to the superior oblique, at the very least, there needs to be a reduction of innervation to the inferior oblique or increased innervation to the superior rectus to account for the changes in torsion in both upward and downward gaze that are consistent with the binocular extension of Listing's law. Prior reports of behavioral and physiological measures of ocular torsion during convergence support this interpretation. Relaxation of the obliques during convergence is suggested by ocular translation (Enright, 1980). Mays, Zhang, Thorsdtad, and Gamlin (1991) demonstrated that convergence-dependent variations of cyclovergence with gaze elevation were associated with a reduced discharge rate of trochlear motor neurons and an implied relaxation of the superior oblique muscle during convergence. The modulation of trochlear activity with convergence varied systematically with gaze elevation, and was largest in downward gaze. The fact that these authors observed no net increase in trochlear activity when the eyes incyclorotate with eye elevation during convergence indicates that the forces of other vertical ocular muscles were modulated during convergence to account for torsional adjustments in upward directions of gaze.

5.4. Vertical alignment in tertiary gaze

Because the obliques and vertical recti are involved in both elevation and torsion, changing the gain of the vertical movers to change torsion might be detrimental for vertical eye alignment. However behavioral measures under open-loop conditions demonstrate that binocular vertical eye alignment is maintained during convergence in tertiary directions of gaze (Collewijn, 1994; Schor et al., 1994; Ygge & Zee, 1995). The contribution of orbital mechanics to maintaining binocular vertical eye alignment during cyclovergence was revealed by the Orbit™ simulation. Vertical eye alignment in the Orbit™ simulation was preserved in tertiary gaze during the gain adjustments to the vertical recti and obliques. Fig. 9 plots the simulated open-loop vertical position of the following eye against closed-loop vertical position of the fixating eye for each of the fifteen fixation points. Results from test positions in all three vertical columns are combined into a single plot. Vertical eye position is specified in Helmholtz coordinates such that a slope of 1.0 (equal vertical position of the following eye and fixating eye) signifies that both eyes were vertically aligned with the fixation target. The top plot shows an amplitude ratio of following over fixating eye of 1.0 indicating that changes in cyclophoria that were consistent with Listing's extended law did not disrupt vertical eye alignment in tertiary gaze. The bottom plot shows a similar amplitude ratio of the two eyes, demonstrating that vertical eye alignment is also achieved during convergence with normal (unaltered) gains to the vertical recti and obliques. In this simulation, the yoked innervation for vertical eye position to the following eye is the same as during distance fixation with parallel lines of sight. The simulation suggests that binocular vertical eye alignment is primarily a consequence of Hering's law and the passive biomechanics of the oculomotor system (Enright, 1992; Miller & Demer, 1992; Porrill, Warren, & Dean, 2000). For normal eye alignment, it is not necessary to postulate a higher level of control to alter the innervation for vertical vergence to obtain binocular alignment of tertiary targets at near and far viewing distances (Ygge & Zee, 1995)

Using Orbit™, we also attempted to model the non-uniform changes in adapted cyclophoria with horizontal gaze direction that we observed following adaptation to the exaggerated condition. Various adjustments of the innervation to vertical ocular muscles did not simulate the non-uniform changes in vertical-cyclophoria gradient with horizontal gaze. Although our simulations demonstrate that the normal and adapted forms of Listing's extended law could be achieved passively with orbital mechanics, without regard for direction of gaze, the non-uniform horizontal spread of cyclovergence aftereffects observed in the exaggerated condition indicates that the oculomotor system has the ability to actively control cyclotorsion using couplings with both direction and distance of gaze. Listing's plane, defined by a uniform spread of aftereffects, could re-emerge with long-term training and adaptation to natural-occurring disparity patterns associated with oculomotor deficits.

This adaptive mechanism could be useful in calibrating K for minor binocular misalignments caused by disturbances of individual extraocular muscles or abnormal coupling between accommodation and convergence that can be reduced with disparity vergence. More extreme alignment anomalies do not always demonstrate normal K values. Melis et al. (1996) demonstrated that the orientation of primary positions

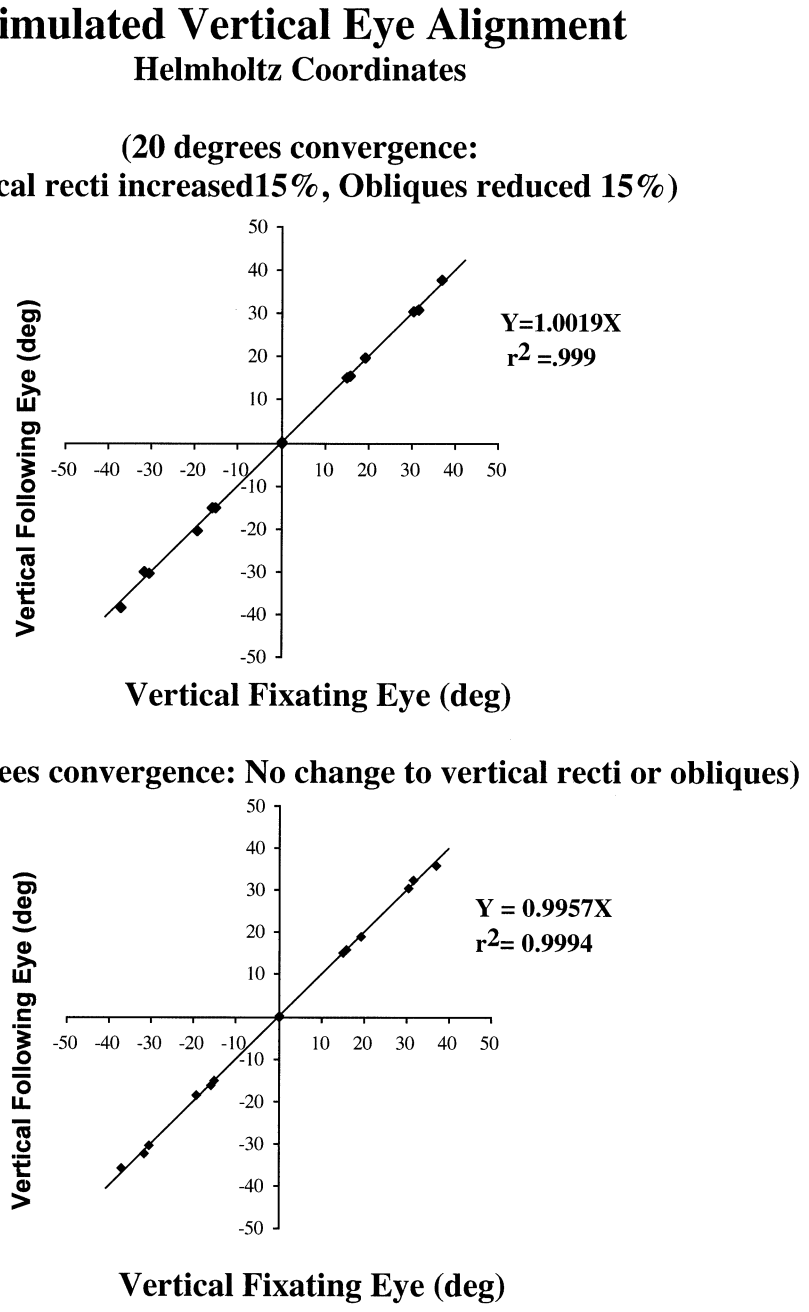

Fig. 9. Simulations of open-loop vertical position of the following eye, is plotted against closed-loop vertical position of the fixating eye for each of fifteen fixation test points. Simulated directions of gaze ranged from the near central fixation point in 30° horizontal increments and 15° vertical increments in a 3×5 rectangular matrix. The Orbit™ simulations are for 20° of convergence with the gain of the obliques decreased by 15% and vertical recti increased by 15% (top) and with a normal (unaltered) set of parameters (bottom).

of a constant esotrope depended on which eye was fixating. In their case report, primary positions did not diverge with accommodative vergence in compliance with Listing's extended law. Instead there was an abnormal coupling between vertical skew of primary positions and convergence. Intermittent exotropes have been shown to have excessive divergence of primary positions during binocular fusion, possibly as a result of extreme convergence efforts (Van den Berg, Van Rijn, & De Faber, 1995). It is possible that sensory anomalies that accompany strabismus may interfere with adaptive processes that would normally calibrate the coupling between convergence and cyclovergence. Most cases of strabismus have a compromised sense of binocular disparity resulting from binocular suppression, amblyopia and/or anomalous retinal correspondence (Schor, 1991). In most cases of strabismus, stereopsis is reduced or absent and there is no need or

visual purpose for a binocular Listing's law. In addition, disparity provides feedback to guide disparity vergence and vergence adaptation. In its absence, the coupling between convergence, vertical gaze and cyclovergence does not appear have access to the feedback necessary for calibration.

Acknowledgements

We wish to thank Joel Miller for his helpful suggestions on running the Orbit™ simulations. We would also like to thank Chris Cantor for developing MATLAB programs for the analysis of rotation vectors. This project was supported by NIH grant no. EYO-3532.

References

Allen, M. J. (1954). The dependence of cyclophoria on convergence, elevation and the system of axes. *American Journal of Optometry*, *31*, 297–307.

Allen, M. J., & Carter, J. H. (1967). The torsion component of the near reflex. *American Journal of Optometry*, *44*, 343–349.

Alpern, M., & Ellen, P. (1956). A quantitative analysis of the horizontal movements of the eyes in the experiments of Johannes Muller. I. Methods and results. *Am. J. Opthalmol.*, *42*, 289–303.

Bruno, P., & Van den Berg, A. V. (1997). Relative orientation of primary positions of the two eyes. *Vision Research*, *37*, 935–947.

Clarke, A. H. (1994). Image processing techniques for the measurement of eye movement. In J. Ygge, & G. Lennerstrand, *Eye movements in reading* (pp. 21–38). Oxford, NY: Elsevier.

Clarke, A. H., Teiwes, W., & Scherer, H. (1991). Videooculography—an alternative method for measurement of three-dimensional eye movements. In R. Schmid, & D. Zambarbieri, *Oculomotor control and cognitive processes*. Amsterdam: Elsevier.

Collewijn, H. (1994). Vertical conjugacy: what coordinate system is appropriate? In A. F. Fuchs, T. Brandt, U. Buttner, & D. S. Zee, *Contemporary ocular motor and vestibular research*: *a tribute to David A. Robinson* (pp. 296–303). Stuttgart: Thieme.

Eadie, A. S., Gray, L. S., Carlin, P., & Mon-Williams, M. (2000). Modeling adaptation effects in vergence and accommodation after exposure to a simulated virtual reality stimulus. *Ophthalmic and Physiological optics*, *20*, 242–251.

Enright, J. T. (1980). Ocular translation and cyclotorsion due to changes in fixation distance. *Vision Research*, *20*, 595–601.

Enright, J. T. (1992). Unexpected role of the oblique muscles in the human vertical fusion reflex. *Journal of Physiology*, *451*, 279–293.

Haslwanter, Th. (1995). Mathematics of three-dimensional eye rotations. *Vision Research*, *35*, 1727–1739.

Haustein, W. (1989). Considerations on Listing's law and the primary position by means of a matrix description of eye position control. *Biological Cybernetics*, *60*, 411–420.

Helmholtz, H. (1962). Movements of the eyes. In J. P. C. Southall, *Helmholtz's treatise on physiological optics*, vol. II (pp. 37–126). New York: Dover.

Hooge, I. T. C., & van den Berg, A. V. (2000). Visually evoked cyclovergence and extended Listing's law. *Journal of Neurophysiology*, *83*(5), 2757–2775.

Howard, I. P., Sun, L., & Shen, X. (1994). Cycloversion and cyclovergence: the effects of the area and position of the visual display. *Experimental Brain Research*, *100*, 509–514.

Judge, S. J., & Miles, F. A. (1985). Changes in the coupling between accommodation and vergence eye movements induced in human subjects by altering the effective interocular separation. *Perception*, *14*, 617–629.

Kertesz, A. E., & Sullivan, M. J. (1978). Effect of stimulus size on human cyclofusional response. *Vision Research*, *18*, 567–571.

Mays, L. E., Zhang, Y., Thorsdtad, M. H., & Gamlin, P. D. R. (1991). Trochlear unit activity during ocular convergence. *Journal of Neurophysiology*, *65*(6), 1484–1491.

Marr, D., & Poggio, T. (1979). A computational theory of human stereo vision. *Proceedings of the Royal Society of London*, *204*, 301–328.

Maxwell, J., & Schor, C. M. (1994). Mechanisms of vertical phoria adaptation revealed by time-course and two-dimensional spatiotopic maps. *Vision Research*, *34*(2), 241–251.

Maxwell J., Graf E., & Schor C. M. (2001). Adaptation of torsional eye alignment in relation to smooth pursuit and saccades. Vision Research, submitted for publication.

McCandless, J. W., & Schor, C. M. (1997). An association matrix model of context-specific vertical vergence adaptation. *Network: Computers and Neural Systems*, *8*, 239–258.

McCandless, J. W., Schor, C. M., & Maxwell, J. (1996). A cross coupling model of vertical vergence application. *IEEE Trans. BioMed Engineering*, *43*, 24–34.

Melis, B., Cruysberg, J., & van Gisbergen, J. (1996). Listing's plane dependence on alternating fixation in a strabismus patient. *Vision Research*, *37*, 1355–1366.

Mikhael, S., Nicolle, D., & Vilis, T. (1995). Rotation of Listing's plane by horizontal, vertical and oblique prism-induced vergence. *Vision Research*, *35*(23/24), 3243–3254.

Miller, J. M., & Demer, J. L. (1992). Biomechanical analysis of strabismus. *Binocular Vision and Eye Muscle Surgery Quarterly*, *7*(4), 233–248.

Miller, J. M., & Robinson, D. A. (1984). A model of the mechanics of binocular alignment. *Computers and Biomedical Research*, *17*, 436–470.

Minken, A. W. H., & van Gisbergen, J. A. M. (1994). A three-dimensional analysis of vergence movements at various levels of elevation. *Experimental Brain Research*, *101*, 331–345.

Mok, D., Cadera, A., Ro, W., Crawford, J. D., & Vilis, T. (1992). Rotation of Listing's plane during vergence. *Vision Research*, *32*, 2055–2064.

Moore, S. T., Haslwanter, T., Curthoys, I. S., & Smith, S. T. (1996). A geometric basis for measurement of three-dimensional eye position using image processing. *Vision Research*, *36*, 445–459.

Porrill, J., Ivins, J. P., & Frisby, J. P. (1999). The variation of torsion with vergence and elevation. *Vision Research*, *39*, 3934–3950.

Porrill, J., Warren, P. A., & Dean, P. (2000). A simple control law generates Listing's positions in a detailed model of the extraocular muscle system. *Vision Research*, *40*, 3743–3758.

Robinson, D. A. (1975). A quantitative analysis of extraocular muscle cooperation and squint. *Investigative Ophthalmology and Visual Science*, *14*, 801–825.

Schor, C. M. (1991). Binocular sensory disorders. In M. Regan, & D. Cronely Jr, *Vision and visual disorders*: *binocular vision*, vol. 9 (pp. 179–224). London: Macmillian Press.

Schor, C. M., Maxwell, J., & Stevenson, S. B. (1994). Isovergence surfaces: the conjugacy of vertical eye movements in tertiary positions of gaze. *Ophthalmic and Physiological Optics*, *14*, 279–286.

Schor, C. M., & McCandless, J. W. (1995a). An adaptable association between horizontal and vertical vergence. *Vision Research*, *35*, 3519–3528.

Schor, C. M., & McCandless, J. W. (1995b). Distance cues for vertical vergence adaptation. *Optometry and Visual Science*, *72*, 478–486.

Schor, C. M., & McCandless, J. W. (1997). Context-specific adaptation of vertical vergence to multiple stimuli. *Vision Research*, *37*, 1929–1938.

Somani, R. A. B., Desouza, J. F. X., Tweed, D., & Vilis, T. (1998). Visual test of listing's law during vergence. *Vision Research*, *38*, 911–923.

Sullivan, M. J., & Kertesz, A. E. (1978). Binocular coordination of torsional eye movements in cyclofusional response. *Vision Research*, *18*, 943–949.

Tweed, D. (1997). Visual-motor optimization in binocular control. *Vision Research*, *37*, 1939–1951.

Tweed, D., & Vilis, T. (1990). Geometric relations of eye position and velocity vectors during saccades. *Vision Research*, *30*, 111–127.

Van Ee, R., & Schor, C. M. (1999). Unconstrained stereoscopic matching of lines. *Vision Research*, *40*, 151–162.

Van den Berg, A. V., Van Rijn, L. J., & De Faber, J. T. H. (1995). Excess cyclovergence in patients with intermittent exotropia. *Vision Research*, *35*, 3265–3278.

Van Rijn, L. J., & Van den Berg, A. V. (1993). Binocular eye orientation during fixations: Listing's law extended to include eye vergence. *Vision Research*, *33*, 691–708.

Van Rijn, L. J., Van der Steen, J., & Collewijn, H. (1994). Instability of ocular torsion during fixation: cyclovergence is more stable than cycloversion. *Vision Research*, *34*, 1077–1087.

Ygge, J., & Zee, D. S. (1995). Control of vertical eye alignment in three-dimensional space. *Vision Research*, *35*, 3169–3181.